Magnetic and radar surveys at Locri Epizephyrii: A comparison between expectations from geophysical prospecting and actual archaeological findings

Magnetic and radar surveys at *Locri Epizephyrii*: a comparison between expectations from geophysical prospecting and actual archaeological findings

C. Colombero[1], D. Elia[2], V. Meirano[2], L. Sambuelli[1]

[1]*Politecnico di Torino, Department of Environment, Land and Infrastructure Engineering, Torino, Italy*
[2]*Università degli Studi di Torino, Department of Historical Studies, Torino, Italy*

The editorial version of this manuscript is available at:

https://www.sciencedirect.com/science/article/abs/pii/S1296207419302973
https://doi.org/10.1016/j.culher.2019.06.012

Abstract

In recent years, geophysical methods have been increasingly applied as a preliminary mapping tool to guide archaeological excavations. Despite the reported growing case histories of geophysical prospections for archaeological purposes, direct comparison between expectations arising from the geophysical results and actual findings is not always systematically performed. A critical comparison between pre-excavation geophysical-guided hypotheses and post-excavation archeological evidences is proposed in this work. A test site within the archaeological area of *Locri Epizephyrii* (Calabria, southern Italy) was chosen for this purpose. An unsurveyed rectangular area (31 x 26 m) was investigated with high-density ground-penetrating radar (GPR) and magnetic profiles. Several anomalous alignments, both compatible and oblique with respect to the orientation of the Greek-Roman city plan, were preliminary observed in the geophysical results. The use of two different techniques allowed for comparison of anomalous areas, enhancing the likelihood of finding features of significance. Two archaeological soundings were later carried out in the areas showing the most peculiar geophysical anomalies. Several structures revealing the same orientation of the ancient city plan and belonging to at least two different building phases were unearthed from a depth of 15-25 cm below the ground surface. A systematic comparison between geophysical and archeological results was then carried out. In general, walls showing different construction typologies (*opus testaceum*, *opus incertum* or *opus caementicium*) were found to generate similar radar anomalies. Artifacts made with materials similar to the background sandy alluvial deposits were not identified by both geophysical techniques, as in the case of an unearthed channel bank, made of local sandstone blocks. GPR was globally observed to detect buried structures better than the magnetic method, probably due to background geological variables linked to the presence of Fe-rich minerals within the background sediments, generating noisier and scattered magnetic gradient maps.

1. Introduction

Geophysical methods have been applied to archaeological prospection since the half of the past century (e.g. [1,2]). With advances in instrumentation and processing techniques, geophysical prospecting is nowadays a largely applied non-invasive tool to investigate archaeological structures. Geophysical methods can be profitably applied as a preliminary mapping tool to guide the archaeological excavations in unknown areas. Even if a dense spatial sampling is needed to obtain high-resolution results, they can cover wide areas with reasonable execution times and costs. A review of the available methods can be found in Linford [3] and Gaffney [4]. A wide variety of successful applications is reported in Piro et al. [5]. Between the available methods, ground-penetrating radar (GPR) can be used for the high-resolution imaging of near-surface targets (e.g. [6-9]). With advances in software and imaging techniques, GPR data interpretation for archaeological purposes is evolving from the analysis of single 2-D profiles to the reconstruction of 3-D volumes, better enabling the spatial tracing of the desired targets [10-12]. High-density magnetic prospecting can be complementary used. Since the magnetic equipment is a portable instrument carried by the user, the method has the advantage of providing a large amount of data in a fast way and on any terrain configuration [13-15]. A proper contrast in electromagnetic and magnetic properties between the artifacts and the surrounding geological conditions is however needed to recover a geophysical signal indicating, above the noise level, the presence of buried structures. A critical comparison between the pre-excavation results of GPR and magnetic prospections and the corresponding archeological findings in presented in this study. An exemplificative geophysical campaign conducted in the archaeological area of *Locri Epizephyrii* is chosen for this purpose.

1.1 Archaeological aspects

The archaeological site of *Locri Epizephyrii* is located in Calabria (southern Italy), on the shore of the Ionic Sea, a few kilometers south of the modern city of Locri (Figure 1). Its millenarian history (see [16]) begins between the end of the 8th and the beginning of the 7th c. BC [17] with the arrival of a group of settlers from Greek motherland. From that moment onwards, the city develops in the course of the ages, from Greek colony to Roman *municipium*, till the unavoidable decline and abandonment by the last inhabitants seeking shelter in the nearby hills, where they founded the new city of Gerace. The University of Turin has been conducting regular excavations at the site since 1969. The explorations mainly focused on the coastal plain of the ancient city, both *intra* and *extra moenia*, and unearthed parts of the Greek fortification system, of the potters' quarter and of the residential area, as well as on two sacred buildings [18-21]. A new research program started in 2002 [22-26] (see also [27-29]) focusing on the central, flat area of the ancient *polis* (6 in Figure 2a), on the seaward side of the so called *Casino Macrì*, a rural building dating to the 18th-19th c. AD, erected on the ruins of a

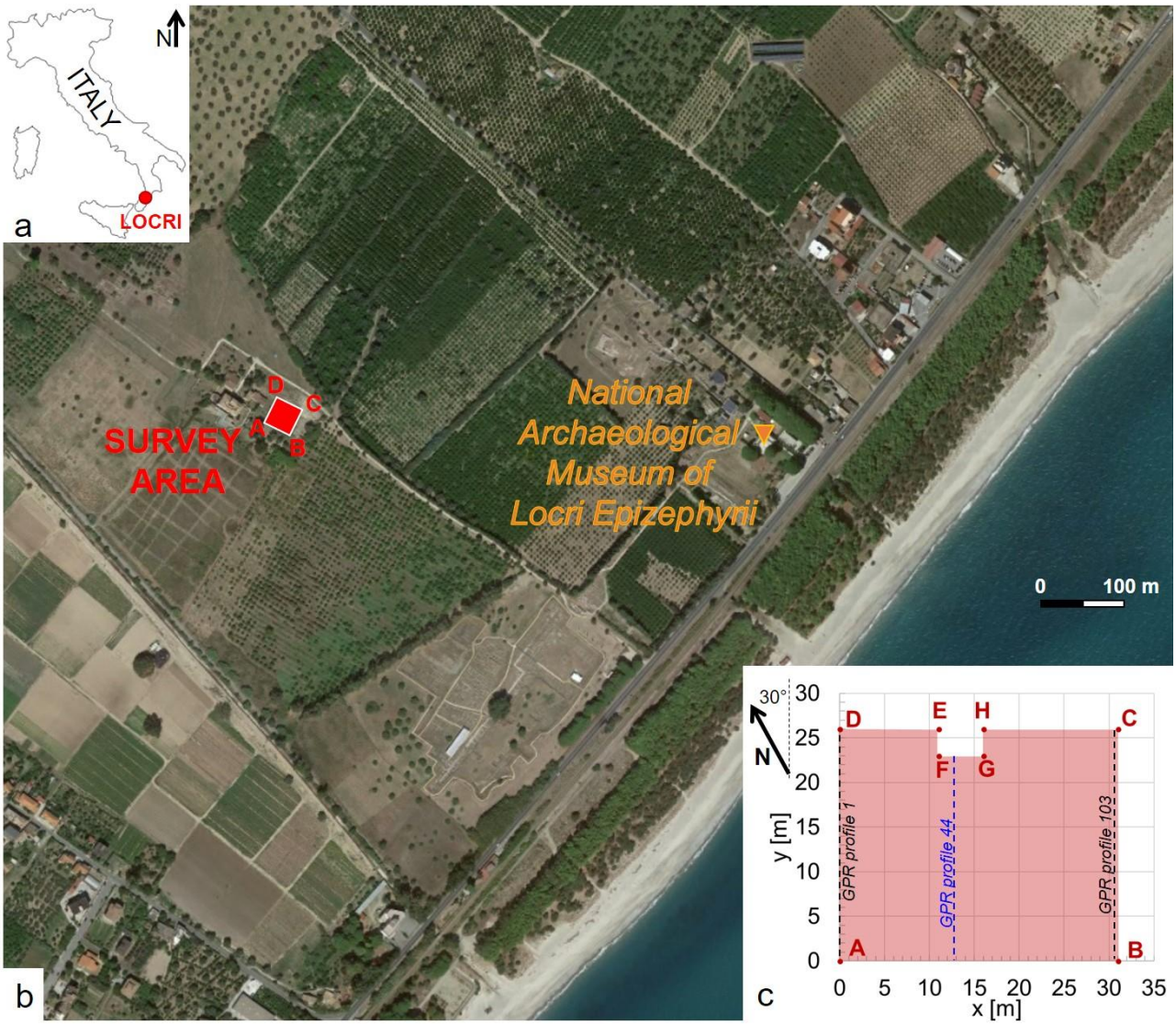

Figure 1 (a) Geographical location and (b) aerial view of the archaeological area of *Locri Epizephyrii*. The area investigated with both geophysical surveys and archaeological excavations is highlighted with the red rectangle. (c) Geometric details of the studied area, with location of some geophysical profiles (black and blue dashed lines) for further analysis of data and results.

Roman imperial thermal complex (2 in Figure 2a). The aim was to acquire new data about the topography and diachronic development of this area, previously neglected by systematic investigation, as well as a more in-depth knowledge about the Roman and post-Roman phases. A complex stratigraphic sequence was in fact brought to light, dating from the foundation of the Greek city to the late antique period. The excavations confirmed the crucial importance of this sector during the entire life span of the site, regarding the water regimentation, the topography and the evolution of the urban fabric. From the origins, the central area of the colony was characterized by the presence of the Milligri (Figure 2a), a seasonal stream descending from a gorge in the highland behind the site, which was responsible for the destruction of the most ancient structures and occupation levels reached

during the excavations, belonging to the 7th c. BC. To regulate water flows and prevent these devastating floods, the Locrians built a monumental channel about 24 m wide (in red in Figure 2b), running from the hill to the sea, dividing the plain area of the city in two parts [23,24,26]. This momentous structure dating to the 6th c. BC, which is unparalleled among Western Greek water regimentation devices so far, influenced the reorganization of the urban space which led to the development of a *per strigas* plan. This grid plan (Figures 2a and Figure 3b) is characterized by long, narrow *insulae* delimited by large road axes approximately parallel to the shore (*plateiai*; 12 m large) and orthogonal narrow cross-streets (*stenopoi*; *circa* 4 m).

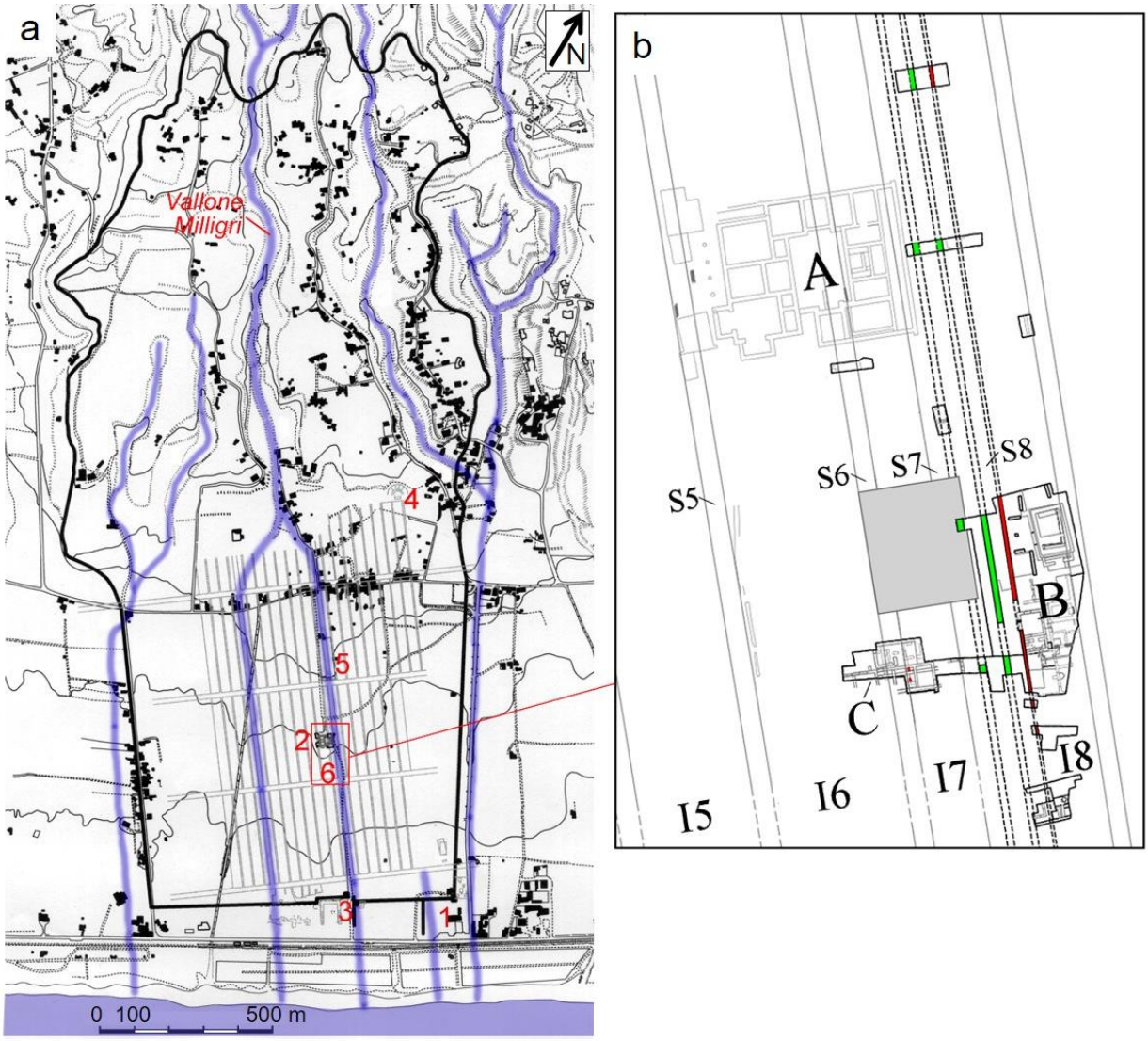

Figure 2 *Locri Epizephyrii*. (a) black bold line: perimeter of the ancient city walls; in blue: ancient streams and channels flowing from NW to SE; 1. National Archaeological Museum; 2. *Casino Macrì* modern building and Roman baths; 3. Aphrodite gate; 4. ancient theatre; 5. Petrara monumental area; 6. area of the recent excavations by the University of Turin. (b) Zoom on the area of the recent excavations by the University of Turin: A. *Casino Macrì* modern building and Roman baths; B. Greek ritual area; C. large late-antique building; I5-I8: ancient *insulae*; S5-S8: ancient *stenopoi* (narrow streets); in red: banks of the Archaic channel; in green: banks of the Classical channel; in grey: area of the geophysical prospections (both modified after Elia [26]).

The central area of the city underwent a radical transformation and space re-shaping during the Classical age, in the first decades of the 4th c. BC [23,26]: the channel was narrowed to less than 7 m (in green in Figure 2b) and flanked by two roads, *stenopoi* S7 and S8; *insula* I7 was created, revealing a complex stratigraphy like *stenopos* S6 and the adjacent *insula* I6, which had been occupied since the Archaic period. A ritual area (B in Figure 2b; [23]) was built in *insula* I8 on the north bank of the Archaic channel, counting a courtyard, a corridor, several rooms, wells and numerous devices related to the ritual use of water. Cult practices are attested by furnishings and votive offerings related to pre-wedding ceremonies and ablutions. The sacred area was in use till the late 3rd c. BC, when the building was suddenly abandoned and the ritual devices intentionally obliterated.

At the end of the 3rd c. BC the bed of the narrow watercourse, with its thick alluvial sediments, was transformed into a small road [24,26]. This radical change affecting the central area of the city is part of the general dismantling and/or modification of the previous water regimentation system, probably due to defensive reasons, as it is attested in various sectors of the city, like the Aphrodite gate near the sea (3 in Figure 2a). The area continues to be occupied until the middle of the 1st c. BC. Afterwards, the meager evidence retrieved and the lack of structures indicate that the street and the houses in the central sector were abandoned.

A renewal started in the 2nd c. AD with the erection of the nearby baths named after the *Casino Macrì* and the construction of further buildings, some of them probably related to the thermal complex, like the pillar-building facing *stenopos* S7 (D in Figure 3a; [24,25]). This sector, together with the Petrara area located west (5 in Figure 2a; [28] pp. 563-567; [25]), becomes now the monumental pole of the Roman imperial city, a period in Locrian archaeology whose knowledge is still far from satisfactory. A further monumental phase is documented during the 3rd and late 4th c. AD [25] when evidence of restructuring and remodeling is known at several areas of the city, like Petrara and the Greek theatre (4 in Figure 2a), which is now transformed in order to serve as an amphitheater. In the central sector of the city, in the southern part of the explored area, a building is erected in this period (in yellow in Figure 3a), later substituted by a new construction, unearthed for at least 22 m (C in Figure 3a), probably corresponding to a public building facing an open space on the west side. These two buildings overlay *insulae* I6 and I7 and *stenopos* S6, and are the first signs in the area of the obliteration and dismantling of the previous urban plan *per strigas*, which had been uninterruptedly respected since the Archaic period [25].

The final occupation phase, between the end of the 5th and the 7th-8th c. AD, is characterized by alternating small residential units and burials accompanied by rare grave goods. The buildings and a short portion of a rudimentary road show a completely divergent orientation in comparison to the previous city plan. Moreover, large scale interventions cut earlier levels and large pits are dug all over

the area, filled with ceramics and debris (Figure 3a). The area previously corresponding to the monumental center of the Roman *municipium* is now transformed in an irregular settlement, as it happens to other sectors of the ancient city like Tribona-Paleapoli and Quote San Francesco (Figure 3b). The site is definitively abandoned by the 8th c. AD.

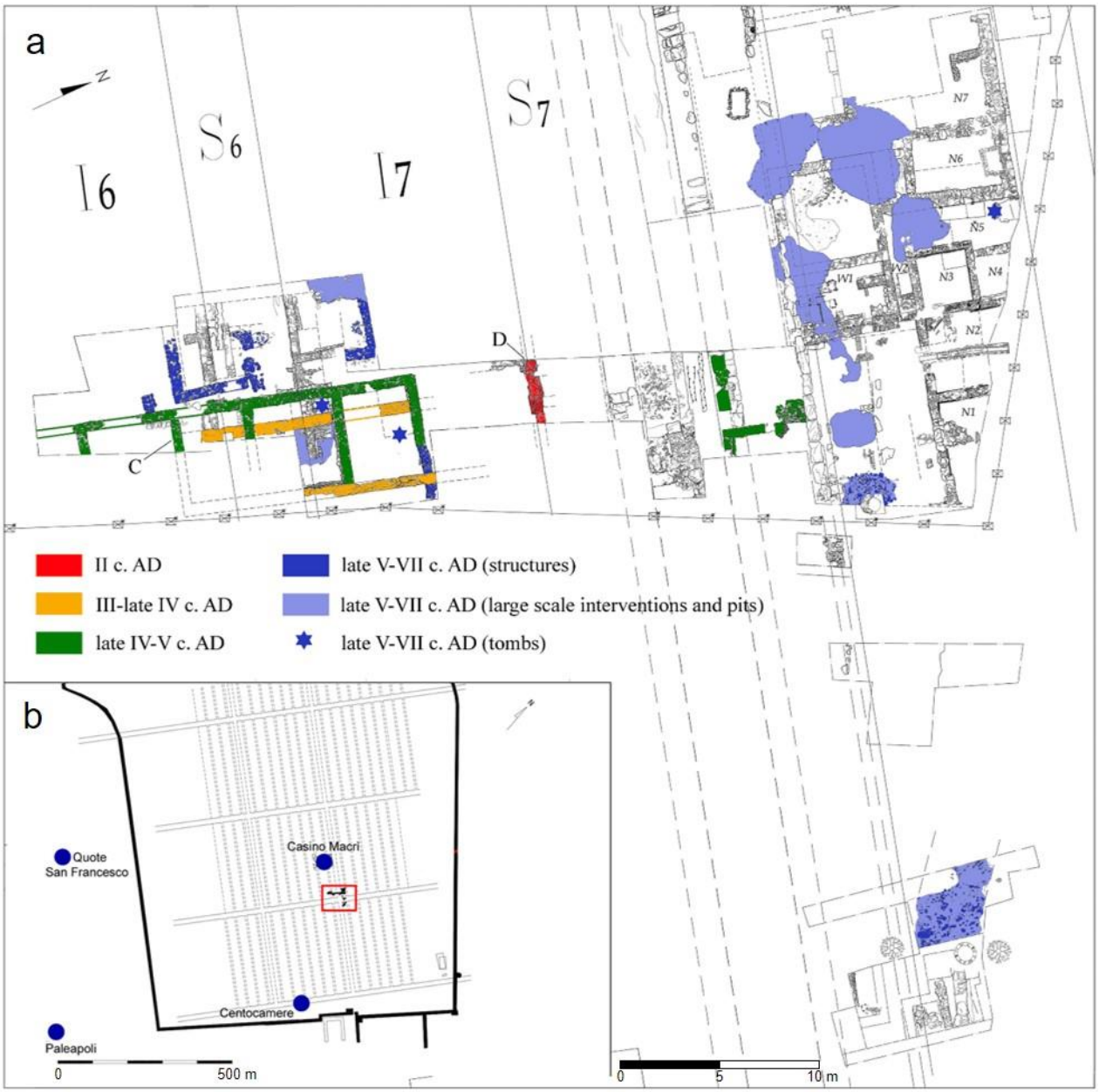

Figure 3 *Locri Epizephyrii*. (a) Detailed map of the area recently excavated by the University of Turin: C. large late-antique building; D. structure pertaining to a pillar building; I6-I7: ancient *insulae*; S6-S7: ancient *stenopoi* (narrow streets. (b) Plain area and perimeter of the ancient city walls (*partim*) with location of the area shown in (a) highlighted with the red rectangle (both modified after Elia et al. [25]).

1.2 Geological setting

In the early stage of the design of a geophysical prospection, a proper analysis of the target and surrounding environment materials is a well-established requirement for a successful investigation [30]. The area of *Locri Epizephyrii* lays on alluvial deposits with different grain size (from clays to gravels) of the *fiumare* (streams) of Gerace and Portigliola, flowing to the north and south of the area respectively. The source area of these small rivers is located in the Aspromonte reliefs. Particularly, plutonic rocks, especially Permian granites, and a heterogeneous sedimentary sequence (conglomerates, sandstones, pelites and clays) starting from the Oligocene to present, are eroded and transported downstream along the river flows. Especially due to the plutonic rocks, significant content in magnetite and Fe-rich minerals within the sediments of the archaeological area, potentially affecting the magnetic survey, could not be *a priori* excluded. In addition, the sedimentary rocks can potentially represent a significant source of clays in the coastal sediments. This aspect can potentially limit the penetration of EM signals for GPR prospecting. Despite this consideration, the grain size of the sediments in the area is prevalently sandy and the water level in the area is deeper than 7 m from the ground floor. These conditions were considered promising for GPR surveying, while the presence of magnetic minerals could not be easily assessed. Nevertheless, also a magnetic survey was attempted.

2 Research aim

Even if geophysical prospecting for archeological purposes is well documented in literature, with a wide variety of case histories, few studies comparing the geophysical results with the actual archaeological findings or trial excavations are present in literature (e.g. [31-34]). Linford and David [35] tried to carry out a semi-quantitative comparison between extensive geophysical surveys (mainly magnetic acquisitions) and later archeological excavations. The availability of simultaneous geophysical measurements and excavations provided the opportunity to attempt an objective comparison on five test sites. Nevertheless, the authors highlighted many limiting factors (e.g. few case studies, variable geology, overburden, topography and surface conditions, recent land-use and seasonality) and problems in data consistency (e.g. spatial sampling and georeferencing of prospections and excavations, variable acquisition parameters, subjective evaluations on data interpretation) preventing a general quantification of the effectiveness of pre-excavation geophysical prospections.

In this work, we focus on the direct comparison between geophysical results and archaeological excavations in order to provide further insight and critical analysis on the relationship between geophysical anomalies and buried structures. The archeological area of *Locri Epizephyrii* is chosen

as test site to conduct this analysis, since a part of the central sector of the area recently investigated by the University of Turin seemed to be particularly promising for geophysical prospections (Figure 1 and Figure 2b). Located between the *Casino Macrì* baths (A in Figure 2a) and the long building unearthed in the southern part of the excavation (C in Figure 2a), it is included in the regular plan of Greek origin and also showed clues of later evidence, belonging to the imperial and late-antique periods.

3 Material and methods

A rectangular area of 806 m^2 (ABCD, Figure 1b and Figure 1c) was selected for GPR and magnetic surveys. The area was referred to a local reference coordinate system (x and y directions in Figure 1c). The y direction of the rectangle is oriented at an angle of N30°E, coincident with the conventional orientation adopted in archaeological literature (e.g. [25]). A small rectangular sector included in the survey area (EFGH) was not investigated due to ongoing archaeological excavations on site. The survey area includes the width of *insula* I7 and *stenopoi* S6 and S7, and its north side approximately corresponds to the expected continuation of the south bank of the channel of Classical age (in green in Figure 2b). The northwest corner is situated near a fragment of an *opus incertum* wall erected on the south limit of the south bank of the channel.

3.1 Geophysical prospecting

3.1.1 GPR survey

The GPR survey was performed with a 500-MHz GSSI antenna connected to a IDS K2 unit. A total of 103 profiles were acquired along the y-direction (Figure 1c) of the investigated rectangle, with a profile spacing (Δx) of 0.3 m. The average trace interval along each profile was 0.03 m, for an average number of about 800 traces along each profile. Traces were acquired at a sampling frequency of 10.24 GHz, for a total recording time of 50 ns.

3.1.2 Magnetic survey

On the same survey area, a magnetic survey was performed with a GSM-19GF Overhauser magnetometer in walking-gradient mode. The Total Magnetic Field (TMF) and the TMF vertical gradient were acquired with lower and upper sensors located respectively at 0.2 m and 0.8 m above the ground surface. A total of 124 magnetic profiles were acquired along the y-direction (Figure 1c) of the investigated rectangle, with a spacing (Δx) of 0.25 m. The acquisition rate was set to 2 readings/s, for an average distance of 0.125 m between subsequent measurements along each profile.

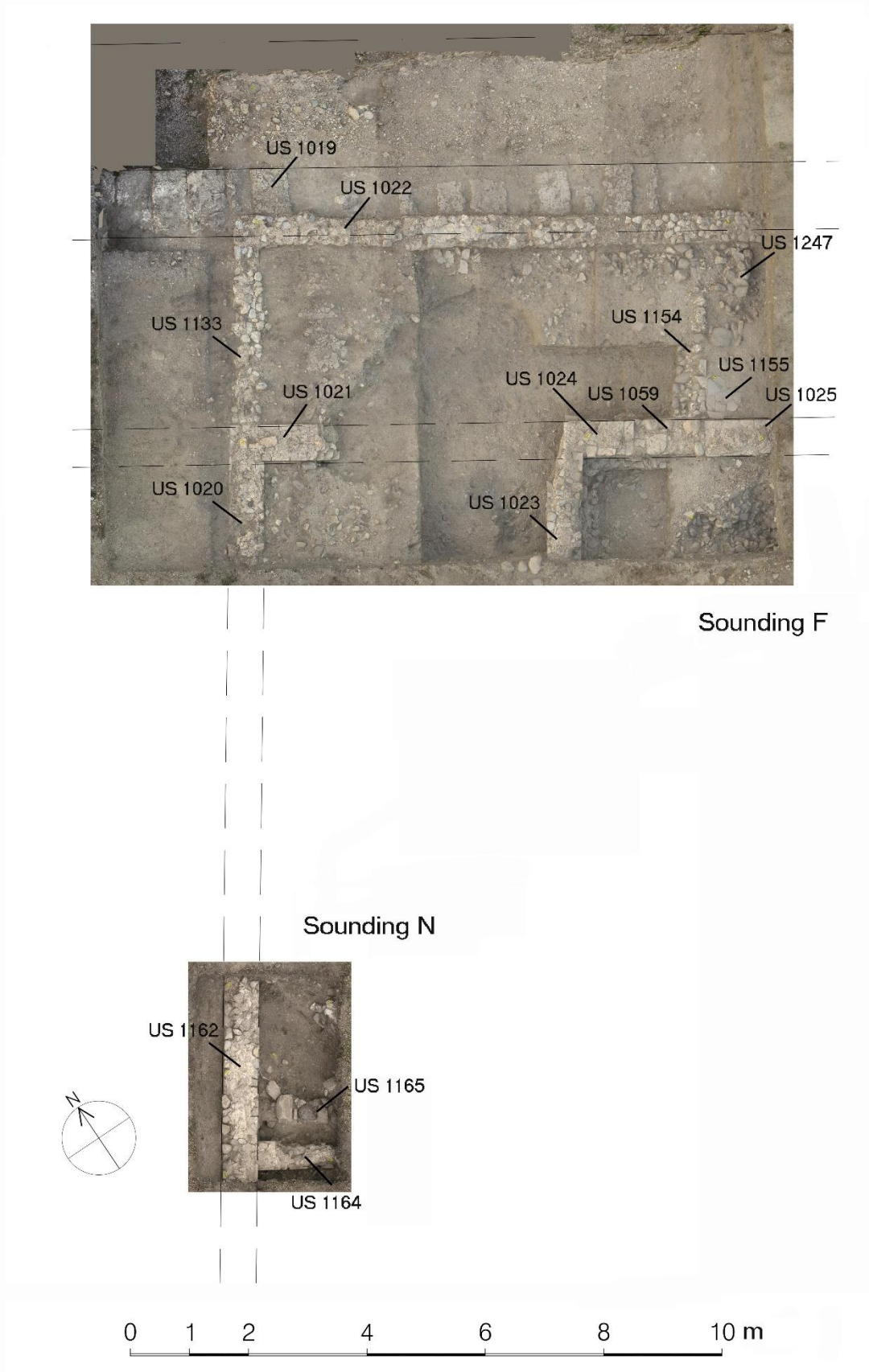

Figure 4 Soundings (F and N) with detail of the unearthed archaeological structures (orthophoto by N. Masturzo, Università degli Studi di Torino, Department of Historical Studies). The elements are labelled with different numbered codes (US=stratigraphic unit). The location of the soundings with respect to the geological prospections is shown in Figure 8.

3.2 Archaeological excavation

A wide sounding (F in Figure 4), measuring 11.50 x 9 m, was opened during the 2017 and 2018 campaigns in the area where both geophysical prospections had shown two sets of orthogonal anomalies. After the removal of modern layers by mechanical means, a few Roman structures bearing mortar emerged at a depth of 15-25 cm. They show the same orientation of the Greek-Roman city plan and belong to at least two different building phases of a monumental construction, recognized on technical and stratigraphic bases. They correspond to the outer walls of the northwest corner and to a few inner walls.

The walls belonging to the first phase (US 1020/1021, US 1023/1024-1059-1025 in Figure 4) measure about 60 cm in width and show *opus testaceum* on the outer side, while the inner side is in *opus incertum*. US 1021 and US 1024-1059-1025 are perfectly aligned and belong to the original north façade of the building. The extant parts reach 30 cm *circa* in height, while the foundations have been only partially investigated.

Two walls in *opus caementicium*, measuring 50-55 cm in width (US 1133 and 1022), belong to the north enlargement of the building. They rise at a higher level in comparison to the previous ones and just preserve their foundations. US 1022, moreover, is directly built on the blocks of US SPA1019, the monumental south bank of the channel dating to the Classical period, and it keeps the same orientation.

Further structures (US 1154, 1155 and 1247) were unearthed in the eastern part of the area delimited by US 1022 and 1025. They are parallel and show north-south orientation.

A smaller sounding (N in Figure 4), measuring 3.50 x 2.50 m, was dug 6.80 m south of F. It partly corresponds to a trench excavated during the Nineties and later filled, where the geophysical prospecting showed a T-shaped anomaly. The excavation brought to light an *opus incertum* north-south structure (US 1162) perfectly aligned to the west outer wall unearthed in sounding F (US 1020, 1133). A perpendicular short structure made in the same technique (US 1164) belongs to the same phase, while a slightly divergent rubble wall (US 1165) is surely later.

4 Results

4.1 GPR results

Raw radargrams were processed with the same processing sequence, involving i) start time moving in correspondence of the main bang (i.e. first reflected GPR pulse) to obtain a correct traveltime, ii) dewow (high-pass filtering to remove electronic noise low-frequency trend), iii) divergence compensation (to recover the amplitude of the deepest reflections), iv) band-pass filter in the range 50-550 Hz (to attenuate noise outside the frequency band of interest), v) background removal

(subtracting the average trace to attenuate the horizontal clutter along the profiles), vi) fitting of the diffraction hyperbola present in the radargrams to estimate the velocity of propagation in the ground, vii) migration of the hyperbola with the average estimated velocity (0.14 m/ns).

An exemplificative GPR section acquired in the center of the investigated area (profile 44, Figure 1c) is shown through the processing sequence (steps i-v) in Figure 5. Even if subtle lateral and vertical variations are already depicted in the processed radargrams, GPR sections were assembled in their 3-D spatial configuration (x, y, time/depth) in order to map and follow the spatial continuity of GPR anomalies in direct comparison with magnetic and excavation results. A volume of GPR data under the investigated area was obtained. Time-slices (Figure 6) were extracted from this volume, with a vertical integration of 1 ns (half-length of the antenna period), to investigate the distribution of the amplitude of reflection (AOR) in maps parallel to the ground surface, corresponding to progressively increasing two-way-times (*twt*), and thus to progressively increasing depths of investigation. Given a constant velocity of propagation (v) of the EM pulse in the investigate subsoil, is indeed straightforward to estimate the depth z related to each time-slice, following:

$$z = \frac{1}{2} twt\ v \qquad (1).$$

Three of the more significant time-slices obtained from the processing of GPR data are shown in Figure 6. The slices are referred to increasing investigation depths. Particularly, considering an average constant velocity of 0.14 m/ns in the shallow subsurface, the depth of each time slice was computed, according to Equation 1, in 0.62 m (Figure 6a), 0.82 m (Figure 6b) and 1 m (Figure 6c) from the ground surface.

The results show a stratified configuration in which recent elements may be present in the shallow subsurface (e.g. alignments of AOR maxima at x<10 m, highlighted with dashed lines in Figure 6d) and disappear at depth.

Peculiar oblique alignments are found in the 0.82-m time slice (dashed lines in Figure 6e). These patterns are not as well defined in the shallower and deeper section (Figure 6d and Figure 6f).

Beside the oblique orientations, sharp orthogonal reflections are present in all the time-slices, from the x-distance of 15 m towards ESE. These high-amplitude patterns show good spatial continuity and seem to delineate concentric rectangular structures. The discontinuity in the AOR may suggest to interpret these anomalies as buried wall summits, laying at variable depths.

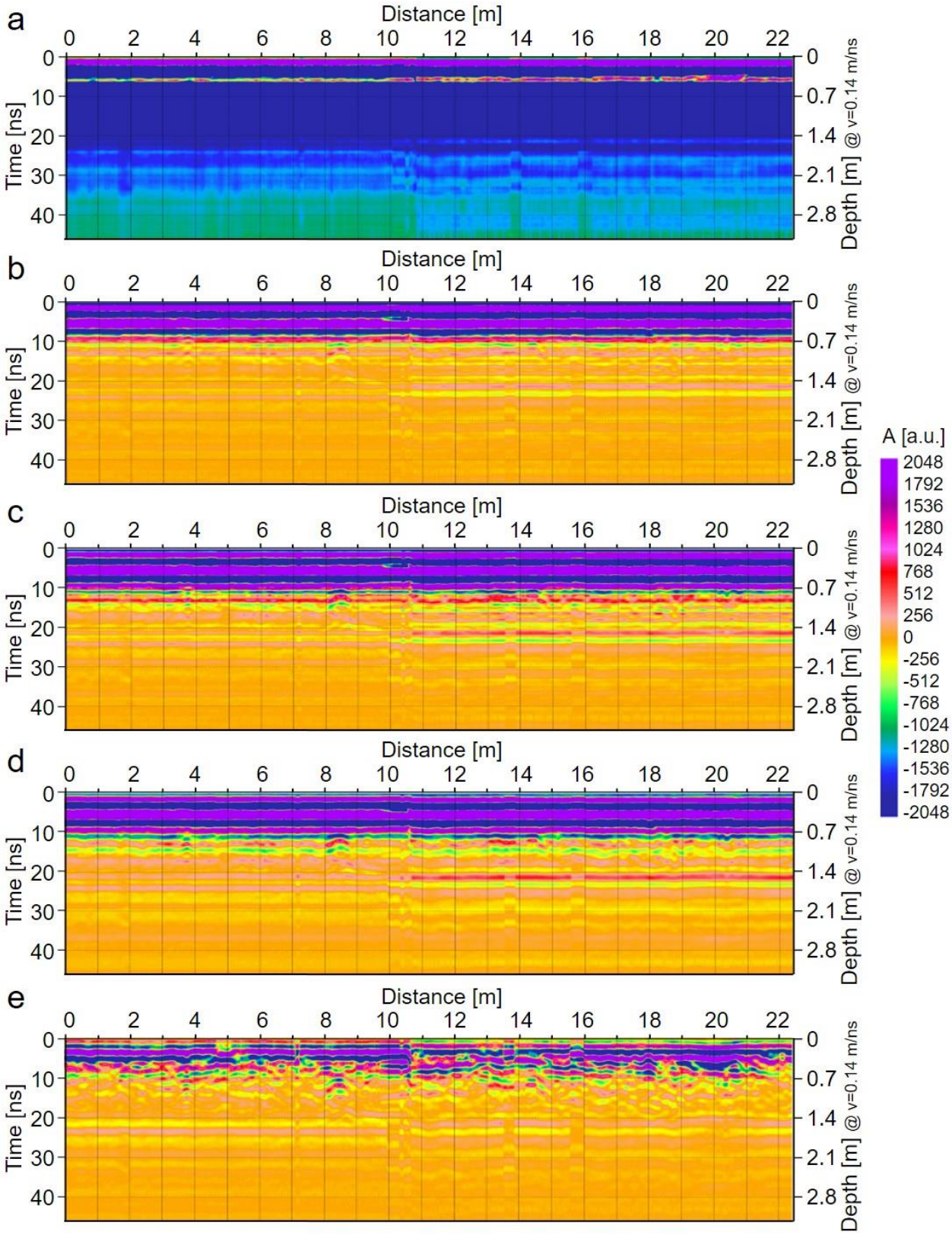

Figure 5 GPR processing sequence on the exemplificative GPR profile 44 (blue dashed line in Figure 1c). Processed radargrams after (a) start time moving, (b) dewow, (c) divergence compensation, (d) band-pass filtering (50-550 Hz), (e) background removal.

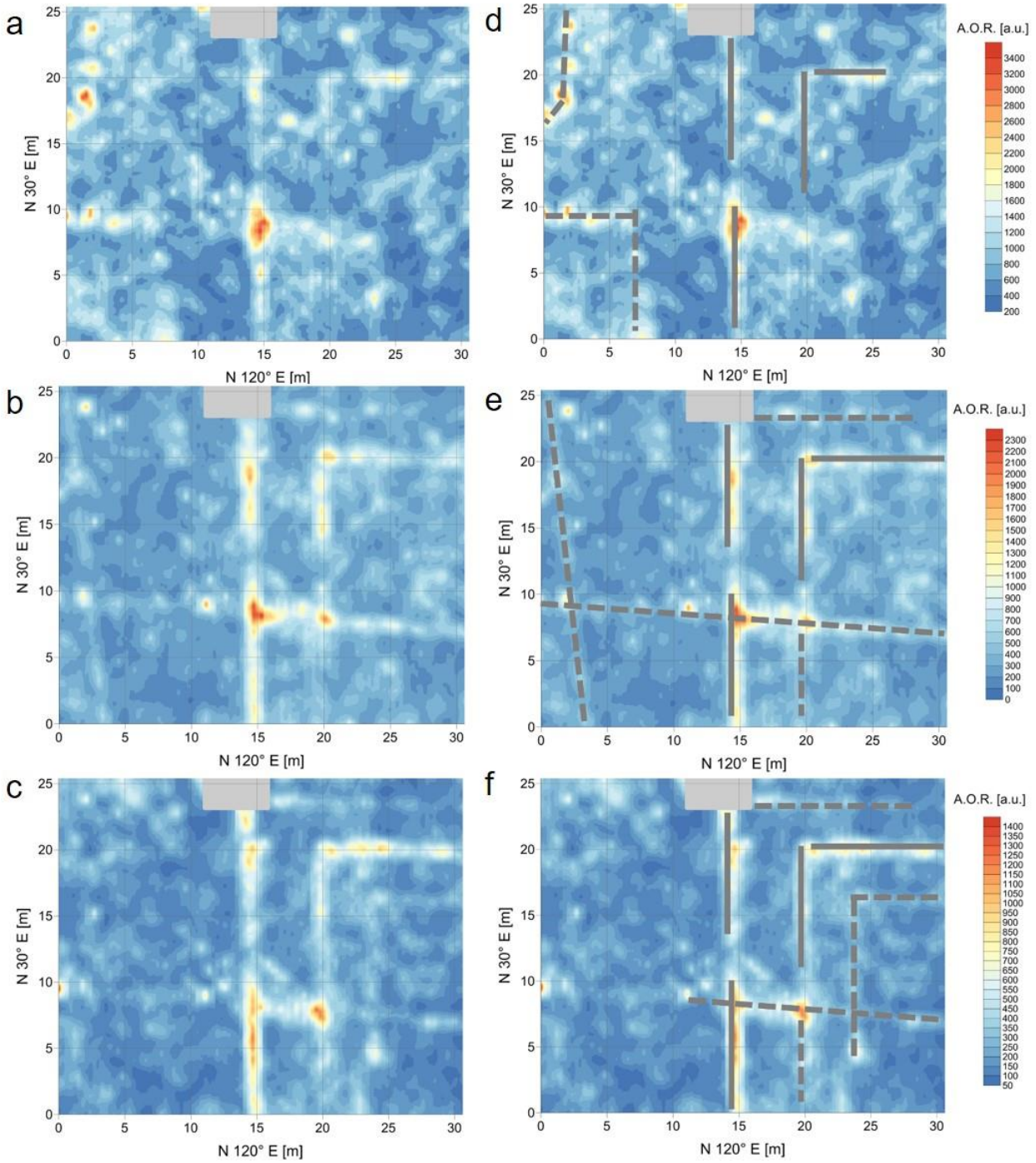

Figure 6 GPR time-slices related to different investigation depths: (a) 0.62 m; (b) 0.82 m; (c) 1 m; (d), (e), (f) are the same of (a), (b) and (c) respectively, with indication of the main reflections (the dashed lines correspond to the most uncertain patterns). In grey: small area explored by archaeologists, inaccessible for geophysical prospections.

4.2 Magnetic results

A total number of 26,600 magnetic measurements were acquired on the survey area. After outlier rejection, only 26,150 high-quality measures were considered for further processing. The gradient map was obtained by means of triangular interpolation over a x-y grid of 0.3 × 0.15 m.

Due to the presence of few localized gradient measurements with high absolute values (>1500 nT/m), possibly hiding lower amplitude gradient fluctuations over the survey area, absolute values higher than 150 nT/m were filtered out. This operation reduced the data set to 25,344 measures (gradient map of Figure 7a and Figure 7b). A further filter, excluding data with absolute value higher than 30 nT/m was finally applied to additionally enhance smaller magnetic anomalies (gradient map of Figure 7c and Figure 7d), reducing the data set to 19,682 measurements. Thanks to the dense initial sampling, after the filter application an average of 26 readings/m^2 was still obtained.

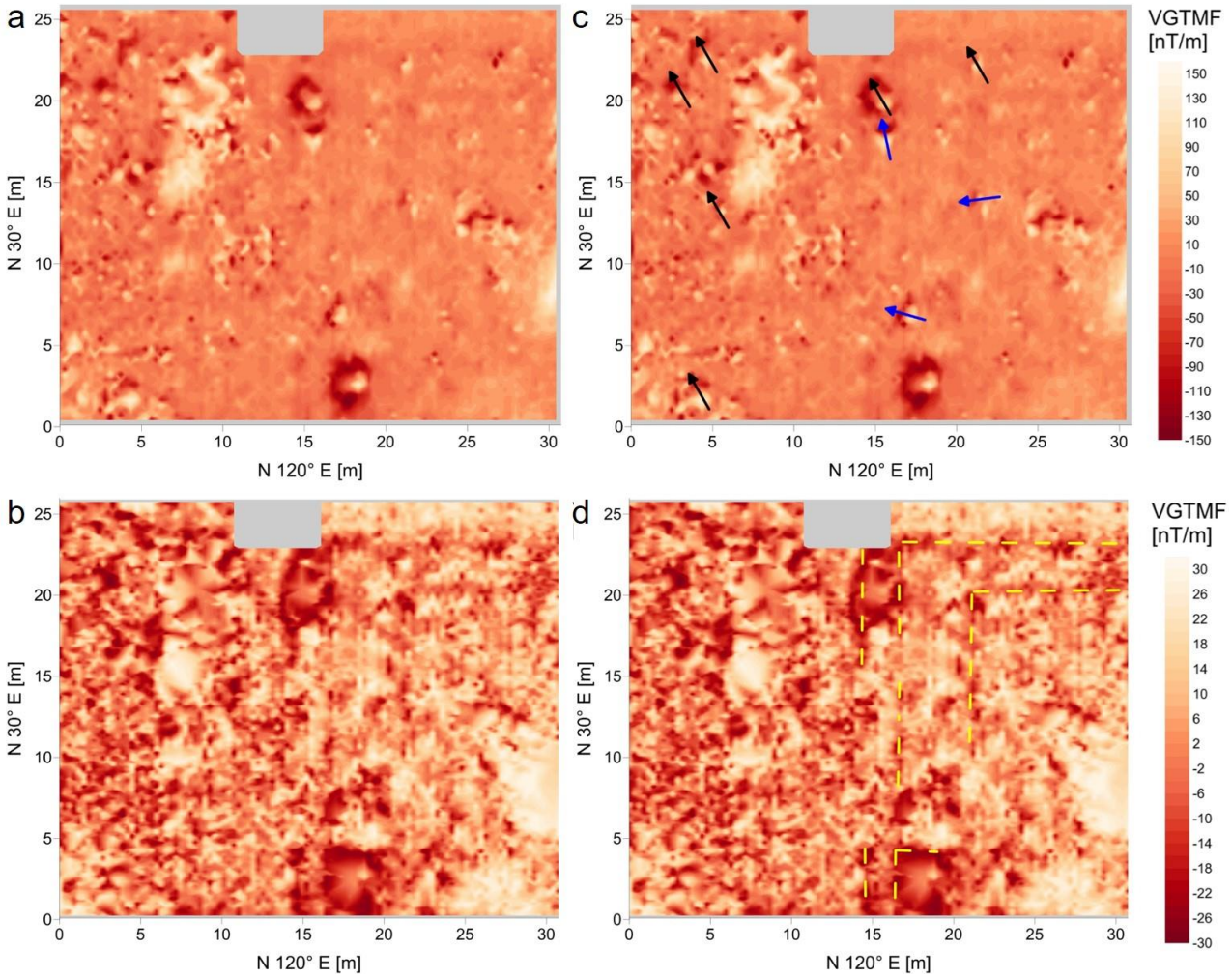

Figure 7 Magnetic gradient maps: (a) measurements with absolute values <150 nT/m; (b) measurements with absolute values <30 nT/m; (c) same map as (a) with indication of the main anomalies attributable to dipoles. Black and blue arrows mark the orientations aligned and not aligned with the present N magnetic pole respectively; (d) same map as (b) with indication of the anomalies possibly attributable to buried structures (the dotted lines correspond to the most uncertain patterns).

The gradients maps obtained from magnetic data processing are reported in Figure 7. The filtered map with absolute values <150 nT/m (Figure 7a) is dominated by a few high-gradient anomalies. Particularly, the two main anomalies (located around x=14 m, y=20 m and x=18 m, y=3 m) may be attributed to shallow bodies with high magnetization and decimetric dimensions. Several anomalies

can be approximately interpreted as magnetic dipoles aligned to the present magnetic N pole (black arrows in Figure 7c). These are probably due to materials which have been magnetized by the Earth's magnetic field, without residual magnetization. Nevertheless, some anomalies show a dipolar configuration with orientation diverging from the present magnetic field (blue arrows in Figure 7c). These orientations suggest the presence of bodies with residual magnetization, not generated from the interaction with the present Earth's magnetic field. The filtered map with absolute values <30 nT/m (Figure 7b) shows diffuse magnetic noise which can be due to the presence of natural material with low-intensity magnetization but strong enough to generate the noisy configuration of the map. Nevertheless, some geometric patterns can be recognized (yellow lines in Figure 7d), globally in agreement with the high-amplitude alignments detected within the GPR time-slices (Figure 6).

5 Discussion

The results of the archeological excavation highlighted a significant coincidence between geophysical anomalies and buried structures. A direct comparison between GPR, magnetic results and archeological soundings in shown in Figure 8. Geophysical anomalies interpreted as possible buried structures before the excavation (right columns of Figure 6 and Figure 7), and effectively corresponding to findings with the same location and orientation, are highlighted with green dashed lines. These include the perpendicular outer walls in the fragments closest to the intersection (US 1022, 1133 and 1020 in Sounding F, Figure 4) for both surveys, while the south continuation of the structure (US 1162 in Sounding N, Figure 4) is depicted only in GPR time slices. No clear magnetic anomalies are found in the area of Sounding N (Figure 8c).

In contrast to successful locations, archeological findings not a-priori identified by any geophysical anomaly are highlighted with the violet lines and shaded areas in Figure 8.

The highest number of these mismatches is found in the magnetic results. Nevertheless, some discrepancies are present also in the GPR time slice. In particular, the alignment of wide sandstone blocks (with size of approximately 0.6 x 0.6 x 1.10 m) forming the south bank of the channel dating to the Classical period (US SPA1019, Figure 4) does not show a different geophysical response with respect to the surrounding material. This can be justified by the weak contrast between the poorly-coherent sandstone blocks and the loose sandy deposits of the background. By contrast, the walls and structures made by stiffer pebbles and clay bricks, cemented by mortar, offer a sharper contrast with the surrounding material. Other minor structures made of the same materials (US 1247, 1154, 1155, 1165, Figure 4), with or without mortar, are however not identified in the geophysical results. The archeological excavations also brought to light fragments of structures whose size was probably too small to sharply appear in a clear geophysical anomaly.

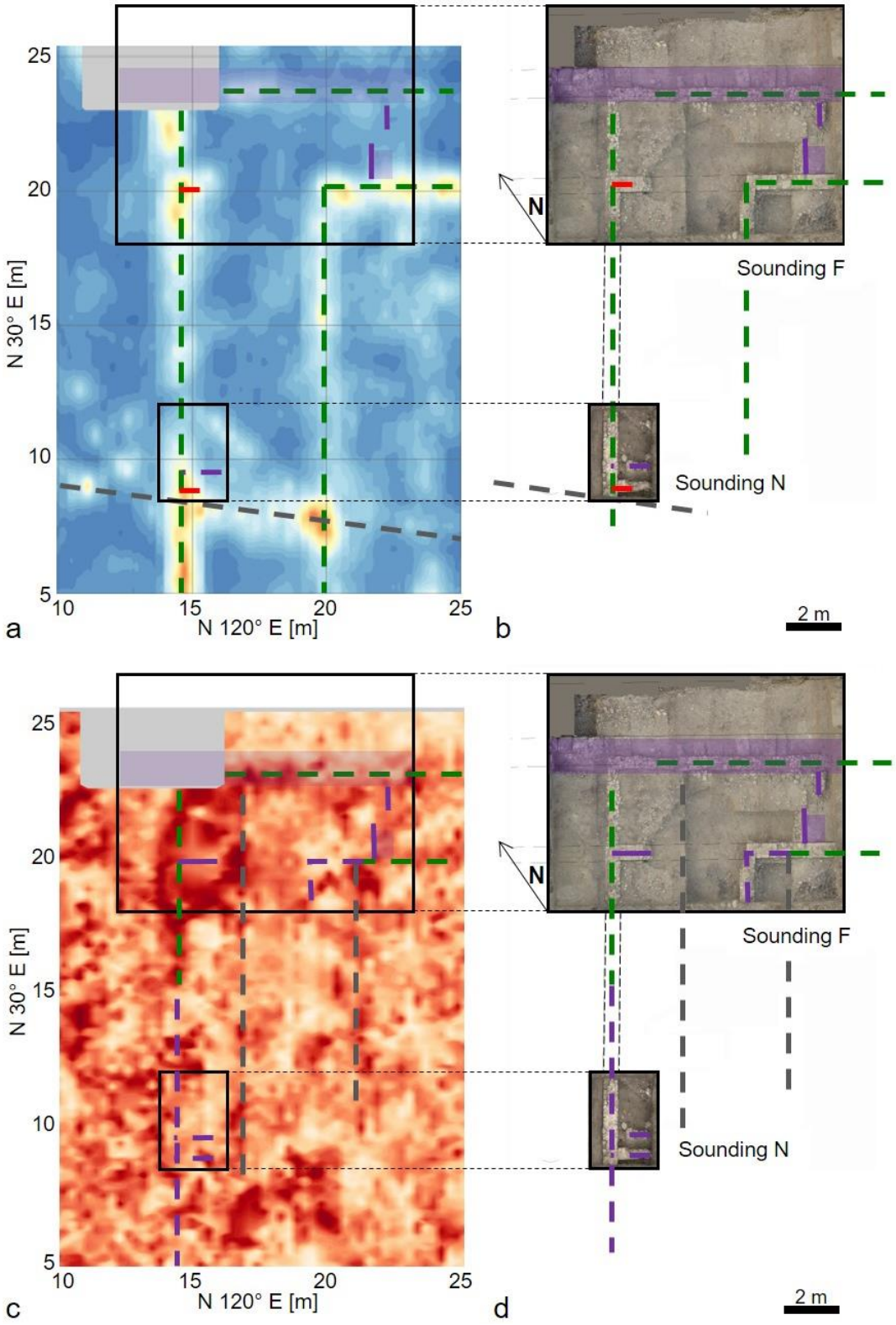

Figure 8 Comparison between geophysical results and archaeological soundings. (a) Zoom on the deeper GPR time slice (Figure 6c and Figure 6f) compared to (b) archaeological structures. (c) Zoom on the magnetic gradient map (measurements with absolute values <30 nT/m, Figure 7c and Figure 7d) compared to (d) archeological structures. In each section, the perimeter of the soundings is delimited by black bold lines. Green line: geophysical anomaly corresponding to a buried structure. Red line: geophysical anomaly not interpreted as a buried structure (but corresponding to). Grey line: geophysical anomaly not corresponding to a buried structure. Violet line and shaded area: buried structure not highlighted as geophysical anomaly.

These elements are highlighted in red in Figure 8. The effect of their presence remained embedded in the anomalies caused by bigger structures (US 1021 in Sounding F, US 1164 in Sounding N, Figure 4). As an example, the main anomaly of US 1020 masks the presence of US 1021 intersection. Even if its presence is quite clear in the GPR slices after comparison with the excavation results (see for example Figure 6b and Figure 6c, where a local maximum in the amplitude of reflection is found at the intersection location), it was not a-priori interpreted as a reliable evidence of a buried object.

Finally, there are geophysical anomalies that were initially interpreted as buried structures but had no validation after the excavation. These features are highlighted with grey dashed lines in Figure 8. In particular, in the magnetic results two anomalous alignments were originally identified as possible structures, parallel to the y-direction of the investigated rectangle and to a set of walls. Their location is not matching with the parallel structures US 1133, 1020 and 1023. The magnetic anomalies seem conversely to highlight a lateral contrast between structures of different height.

No structures clearly related to the oblique GPR anomaly intersecting the SW corner of Sounding N were found during the excavation. This peculiar alignment of maxima in amplitude of reflection can be related to deeper structures and is however located at the limit of the excavated area.

The relative depth of the different structures highlighted in the GPR time slices was generally confirmed during the archaeological excavation. Progressively going deeper, the imprint of shallow later structures was coherently found to disappear in the geophysical results. Some discrepancies in quantitative depth estimation between time slices and field conditions were however observed. This difference is probably due to the heterogeneous site velocities, slightly varying both laterally and vertically, with respect to the uniform velocity adopted for time-to-depth conversion.

No clear relationship between the construction typologies recognized in the soundings (*opus testaceum*, *incertum* and *caementicium*) and the intensity of the geophysical anomalies was established.

6 Conclusions

A direct comparison between geophysical prospections and archeological excavations was carried out in this work, with the aim of verifying the correspondence between expectations and actual findings and analyzing the possible influence of materials and construction typologies on radar and magnetic data. A promising research sector was identified as a test site within the archaeological area of *Locri Epizephyrii* (southern Italy). A rectangular surface (width=31 m, length=26 m) was covered with high-density GPR and magnetic profiles. The use of two different geophysical techniques allowed for comparison of anomalous areas, enhancing the likelihood of finding features of significance. Several anomalous alignments, both compatible and oblique with respect to the

orientation of the Greek-Roman city plan, were preliminary observed in GPR time slices and magnetic gradient maps. These geophysical results guided the location of two archaeological soundings in sectors of the investigated rectangle showing the most peculiar geophysical anomalies. Several structures showing the same orientation of the ancient city plan and belonging to at least two different building phases were found from a depth of 15-25 cm. Walls belonging to the first phase showed *opus testaceum* and *opus incertum* on the outer and inner side respectively. A perfect alignment of the wall fragments was observed between the two soundings, suggesting a continuous structure. Two walls in *opus caementicium* belonging to the second phase correspond to an enlargement of the building. All these wall structures, independently from the construction typology, were correctly identified by GPR anomalies, while the magnetic gradient map only partially located these structures within the larger archaeological sounding. Further minor structures, unearthed in the eastern part of the main sounding, despite the similar construction typology, showed no evidence on the geophysical results. This can be probably interpreted as due to the small dimensions and different orientations of these targets in a small area, generating therefore a less clear contrast with the surrounding materials if compared with the other detected walls.

The monumental south bank of the Classical channel, formed by an alignment of big sandstone blocks running parallel to one of the wall elongations, was disclosed in the same sounding. Also in this case, the weak contrast between the poorly-coherent sandstone blocks and the loose sandy deposits of the background did not generate GPR or magnetic signals which could be classified as anomalies.

The GPR results were globally found to better highlight the buried structures with respect to the noisy magnetic data, probably due to background geological variables linked to the presence of Fe-rich minerals within the alluvial sediments of the site.

Acknowledgments

The authors are sincerely grateful to Diego Franco for the help in geophysical data acquisition.

References

[1] E. Segre, Mezzi tecnici ausiliari nella prospezione archeologica: Lerici, Roma, 1958.

[2] A.I. Rees, Electrical prospecting method in archaeology, Antiquity 36 (132) (1962) 131-134.

[3] N. Linford, The application of geophysical methods to archaeological prospection, Rep. Prog. Phys. 69 (2006) 2205-2257.

[4] C. Gaffney, Detecting trends in the prediction of the buried past: a review of geophysical techniques in archaeology, Archaeometry 50 (2008) 313-336.

[5] S. Piro, S. Negri, T. Quarta, M. Pipan, E. Forte, M. Ciminale, E. Cardarelli, P. Capizzi, L. Sambuelli, Geophysics and cultural heritage: a living field of research for Italian geophysicists, First Break 33 (8) (2015) 43-54.

[6] M. Pipan, L. Baradello, E. Forte, A. Prizzon, I. Finetti, 2-D and 3-D processing and interpretation of multi-fold ground penetrating radar data: a case history from an archaeological site, Journal of Applied Geophysics 41 (1999) 271-292.

[7] A. Ates, Archaeogeophysical Investigations around the Bilge Qagan Monument in Khosho Tsaidam, Mongolia, Archaeological Prospection 9 (2002) 23-33.

[8] S. Piro, D. Goodman, Y. Nishimura, The study and characterization of Emperor Traiano's Villa (Altopiani di Arcinazzo-Roma) using high-resolution integrated geophysical surveys, Archaeological Prospection 10 (2003) 1-25.

[9] S. Piro, I. Haynes, P. Liverani, D. Zamuner, GPR investigation to map the subsoil of the St. John Lateran Basilica (Rome, Italy), Bollettino di Geofisica Teorica ed Applicata 58 (4) (2017) 431-444.

[10] L. Nuzzo, G. Leucci, S. Negri, M.T. Carrozzo, T. Quarta, Application of 3D visualization techniques in the analysis of GPR data for archaeology, Annals of Geophysics 45 (2) (2002) 321-338.

[11] M. Bini, A. Fornaciari, A. Ribolini, A. Bianchi, S. Sartini, F. Coschino, Medieval phases of settlement at Benabbio castle, Apennine mountains, Italy: evidence from ground penetrating radar survey, Journal of Archaeological Science 37 (12) (2010) 3059-3067.

[12] W. Zhao, E. Forte, S.T. Levi, M. Pipan, G. Tian, Improved high-resolution GPR imaging and characterization of prehistoric archaeological features by means of attribute analysis, Journal of Archaeological Science 54 (2015) 77-85.

[13] R.E. Chavez, M.C. Hernandez, J. Herrera, M.E. Camara, A magnetic survey over La Maja, an archaeological site in Northern Spain, Archaeometry 37 (1995) 171-184.

[14] P. Crew, Magnetic mapping and dating of prehistoric and medieval iron-working sites in northwest Wales, Archaeological Prospection 9 (3) (2002) 163-182.

[15] N. Abrahamsen, B.H. Jacobsen, U. Koppelt, P. de Lasson, T. Smekalova, O. Voss, Archaeomagnetic investigations of Iron Age slags in Denmark, Archaeological Prospection 10 (2) (2003) 91-100.

[16] L. Costamagna, C. Sabbione, Una città in Magna Grecia. Locri Epizefiri. Guida Archeologica, Reggio Calabria, 1990.

[17] D. Elia, V. Meirano, Locri Epizefiri. Nuovi scavi dell'Università di Torino, in: Alle origini della Magna Grecia. Mobilità, migrazioni, fondazioni. Atti del L Convegno di Studi sulla Magna Grecia (Taranto, 1-4 ottobre 2010), Taranto, 2012, pp. 847-854.

[18] M. Barra Bagnasco, Locri Epizefiri I, Firenze, 1977.

[19] M. Barra Bagnasco, Locri Epizefiri II. Gli isolati I2 e I3 dell'area di Centocamere, Firenze, 1989a.

[20] M. Barra Bagnasco, Locri Epizefiri III. Cultura materiale e vita quotidiana, Firenze, 1989b.

[21] M. Barra Bagnasco, Locri Epizefiri IV. Lo scavo di Marasà Sud. Il sacello tardo arcaico e la «casa dei leoni», Firenze, 1992.

[22] M. Barra Bagnasco, Ancora sull'impianto urbano di Locri Epizefiri: una nota alla luce di recenti scoperte, Orizzonti III (2002) 89-97.

[23] D. Elia, V. Meirano, Il sacro e l'acqua a Locri Epizefiri: osservazioni alla luce delle scoperte recenti, in: A. Russo, F. Guarneri (Eds.), Santuari mediterranei tra Oriente e Occidente. Interazioni e contatti culturali, Atti del Convegno Internazionale (Civitavecchia-Roma, 2014), Roma, 2016, pp. 419-434.

[24] D. Elia, V. Meirano, Locri Epizefiri. Al cuore dell'antica città. Vecchi problemi e nuove scoperte, dalla fondazione all'età romana, in: A. Pontrandolfo, M. Scafuro (Eds.), Dialoghi sull'archeologia della Magna Grecia e del Mediterraneo, Atti del I Convegno Internazionale di Studi (Paestum, 7-9 settembre 2016), tomo II, Paestum, 2017, pp. 265-274.

[25] D. Elia, V. Meirano, A. Colonnetta, Locri Epizefiri (RC). Nuovi dati sui modi dell'abitare in età tardoantica, in: I. Baldini, C. Sfameni (Eds.), Abitare nel Mediterraneo tardoantico, Atti del II Convegno Internazionale del Centro Interuniversitario di Studi sull'edilizia abitativa tardoantica nel Mediterraneo CISEM (Bologna, 2-5 marzo 2016), Bari, 2018, pp. 167-173.

[26] D. Elia, La gestione delle acque a Locri Epizefiri. Criticità e soluzioni, dalle origini alla conquista romana, in: O. Belvedere, S. Bouffier, S. Vassallo (Eds.), Installations hydrauliques et gestion de l'eau en Méditerranée au 1er millénaire avant notre ère, Actes Hydromed Symposium II (Palerme 3-5 décembre 2015), Aix en Provence, forthcoming.

[27] S. Bonomi, La Calabria, in: Alle origini della Magna Grecia. Mobilità, migrazioni, fondazioni. Atti del L Convegno di Studi sulla Magna Grecia (Taranto, 1-4 ottobre 2010), Taranto, 2012, pp. 1405-1449.

[28] S. Bonomi, La Calabria, in: Da Italìa a Italia. Le radici di un'identità. Atti del LI Convegno di Studi sulla Magna Grecia (Taranto, 29 settembre-2 ottobre 2011), Taranto, 2014, pp. 541-584.

[29] S. Bonomi, La Calabria, in: Poleis e politeiai nella Magna Grecia arcaica e classica. Atti del LIII Convegno Internazionale di Studi sulla Magna Grecia (Taranto, 26-29 settembre 2013), Mottola, 2016, pp. 603-647.

[30] L. Sambuelli, C. Strobbia, The Buffon needle problem and the design of a geophysical survey, Geophysical prospecting 50 (4) (2002) 403-409.

[31] G.N. Tsokas, A. Giannopoulos, P. Tsourlos, G. Vargemezis, J.M. Tealby, A. Sarris, C.B. Papazachos, T. Savvopoulou, A large scale geophysical survey in the archaeological site of Europos (N. Greece), Journal of Applied Geophysics (32) (1994) 85-98.

[32] V. Basile, M.T. Carrozzo, S. Negri, L. Nuzzo, T. Quarta, A.V. Villani, A ground-penetrating radar survey for archaeological investigations in an urban area (Lecce, Italy), Journal of Applied Geophysics 44 (1) (2000) 15-32.

[33] S. Campana, M. Dabas, L. Marasco, S. Piro, D. Zamuner, Integration of remote sensing, geophysical surveys and archaeological excavation for the study of a medieval mound (Tuscany, Italy), Archaeological Prospection 16 (2009) 167-176.

[34] G. El-Qady, M. Metwaly, Archaeogeophysics. State of Art and Case Studies, 1st ed., Springer Publishing Company, Incorporated, Heidelberg, 2018.

[35] N. Linford, A. David, Study of geophysical surveys, in: G. Hey, M. Lacey (Eds.), Evaluation of archaeological decision-making processes and sampling strategies, Canterbury, Kent County Council, pp. 76-89.